

## Self-similar asymptotics in convergent viscous gravity currents of non-Newtonian liquids

This content has been downloaded from IOPscience. Please scroll down to see the full text.

2009 J. Phys.: Conf. Ser. 166 012011

(<http://iopscience.iop.org/1742-6596/166/1/012011>)

View [the table of contents for this issue](#), or go to the [journal homepage](#) for more

Download details:

IP Address: 157.92.4.72

This content was downloaded on 18/08/2015 at 17:50

Please note that [terms and conditions apply](#).

# Self-similar asymptotics in convergent viscous gravity currents of non-Newtonian liquids

Julio Gratton<sup>1</sup> and Carlos Alberto Perazzo<sup>2</sup>

<sup>1</sup> INFIP-CONICET, Dpto. de Física, FCEyN, UBA, Ciudad Universitaria, Pab. I, 1428 Buenos Aires, Argentina.

<sup>2</sup> Universidad Favaloro and CONICET, Solís 453, 1078 Buenos Aires, Argentina.

E-mail: jgratton@tinfiplfp.uba.ar, perazzo@favaloro.edu.ar

**Abstract.** We investigate the evolution of the ridge produced by the convergent motion of two substrates, on which a layer of a non-Newtonian power-law liquid rests. We focus on the self-similar regimes that occur in this process. For short times, within the linear regime, the height and the width increase as  $t^{1/2}$ , independently of the rheology of the liquid. In the self-similar regime for large time, the height and the width of the ridge follow power laws whose exponents depend on the rheological index.

## 1. Introduction

Mountain belts arise due to the shortening of the crust that occurs when two lithospheric plates collide, or when a plate is subducted beneath an other. However there is also abundant geological evidence showing that extension occurs in the central part of many mountain belts, notwithstanding shortening is taking place. This apparently paradoxical fact suggested one of us [1] the idea that mountain building occurs as a consequence of a dynamic balance between the shortening of the plate and the spreading flow, that occurs because an isostatically compensated range is not in hydrostatic equilibrium, and tends to spread and collapse unless restrained by appropriate stresses. Indeed, it can be easily estimated that the characteristic time for the collapse of a mountain range resulting from root spreading is of the same order of magnitude as the times involved in orogeny, which means that both processes (shortening and lateral spreading) occur simultaneously. Starting from these considerations the scaling laws for the evolution of orogenic belts were derived, based on simple physical hypotheses about the viscous flow caused by the shortening of the Earth's crust [1], which is assumed to have a velocity that depends on the depth.

Various physical models have been used to simulate the build-up and the evolution of mountain belts. All are extensions and variations of the thin viscous sheet model of England and McKenzie [2; 3]. A discussion and a classification of these models has been made by Medvedev and Podladchikov [4; 5], to which the reader is referred for more details. All these numerical calculations attempt to describe specific orogenies as realistically as possible. No effort has been made to gain a deeper physical insight of the process. In particular no scaling laws have been derived from these models. Unlike in [1] most thin viscous sheet models assume that the velocity field does not depend on the vertical coordinate, so that the main gradient is horizontal. It was

shown in [1] that this assumption leads to scaling laws that are slightly different from those derived under the assumption that the main velocity gradient is vertical.

To achieve a better understanding about these kind of flows we investigated a simple model that consists of an initially uniform fluid layer that rests over an horizontal substrate. This substrate is divided in two parts, that for  $t > 0$  are pushed one against the other [6]. This convergent motion drags the liquid, and produces a ridge (see figure 1). We studied the evolution of the flow of a Newtonian liquid, and we showed that there are two self-similar regimes that occur in different space-time domains. These regimes and their corresponding scaling laws were obtained analytically. Here we extend these results for liquids with a power-law rheology, because this behavior is more appropriate to describe the behavior of the lithosphere.

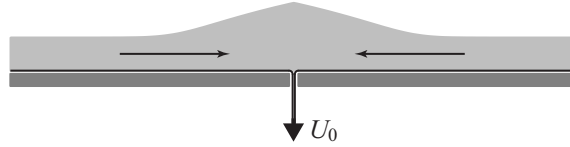


**Figure 1.** Formation of a ridge due to the convergent motion of the substrates.

## 2. Basic equations

The geometry of our model is shown in figure 1: an initially uniform liquid layer rests on two substrates, that start to move suddenly with velocities  $U_0 > 0$  (the substrate for  $X < 0$ ) and  $-U_0$  (the substrate for  $X > 0$ ). Thanks to the symmetry of the problem it is enough to consider the half-plane  $X > 0$ . Then we assume that a uniform semiinfinite liquid layer, whose thickness is  $H_0$ , rests on a rigid horizontal surface, and that at  $X = 0$  there is a vertical wall over which the liquid slips. At  $T = 0$  the substrate starts to move with the constant speed  $-U_0$  so that the liquid accumulates against the wall. We assume a power-law rheology of the form

$$\tau_{ij} = AE^{(1-n)/n} \dot{\epsilon}_{ij}, \quad E = (\dot{\epsilon}_{ij} \dot{\epsilon}_{ij})^{1/2}. \quad (1)$$

Here  $\tau_{ij}$  and  $\dot{\epsilon}_{ij} = \frac{1}{2}(\partial_j v_i + \partial_i v_j)$  are the components of the stress and the strain rate tensors, and  $A$ ,  $n$  are positive constants. A Newtonian liquid corresponds to  $n = 1$ , in which case the viscosity is  $A/2$ . Reasonable values for the lithosphere are  $n = 3$  and  $A = 10^{13}$  (c.g.s) [7]. We assume that the flow is slow and dominated by shear stresses, so we can employ the lubrication approximation [8] (we neglect surface effects). Let  $H \equiv H(X, T)$  be the thickness of the layer, and  $U \equiv U(X, T)$  its vertically averaged horizontal velocity. The boundary conditions are  $U(0, T) = 0$  and  $H(\infty, T) = H_0$ . We define the dimensionless variables  $u$ ,  $h$ ,  $x$ ,  $t$  by means of

$$U = U_0 u, \quad H = H_0 h, \quad X = X_0 x, \quad T = \frac{X_0}{U_0} t,$$

where

$$X_0 = \frac{\rho g}{A} \left[ \frac{2^{\frac{1+n}{2}} H_0^{2n+1}}{(n+2)U_0} \right]^{\frac{1}{n}},$$

$g$  is the acceleration of gravity and  $\rho$  is the density of the liquid. The evolution equation is then

$$h_t = h_x + s (h^{n+2} |h_x|^n)_x, \quad s \equiv \text{sign}(h_x). \quad (2)$$

This equation can be written as the continuity equation

$$h_t = -(uh)_x, \quad (3)$$

where

$$u = -1 - s h^{n+1} |h_x|^n, \quad (4)$$

is the dimensionless vertically averaged horizontal velocity. In the case we are considering  $s = -1$ , then the initial and boundary conditions are

$$h(x, 0) = 1, \quad h(\infty, t) = 1, \quad h^{1+\frac{1}{n}} h_x \Big|_{x=0} = -1. \quad (5)$$

The second of these conditions implies that for large  $x$ , where  $h_x \rightarrow 0$ , the velocity is essentially equal to that of the substrate. The third condition implies that  $u(0, t) = 0$ , which means that at  $x = 0$  the nonlinear diffusion term in (4) exactly cancels the advective term. On the other hand, from mass conservation one has  $\int_0^\infty (h - 1) dx = t$ . Then we see that the accumulation of mass near  $x = 0$  due to advection is counteracted by the diffusion produced by gravity. Notice that the boundary condition at  $x = 0$  depends on the rheology, and that as  $n$  increases the ridge tends to have a steeper peak.

### 3. Numerical solutions

The problem (2-5) does not have a closed solution. We show some numerical results in figures 2 and 3. Figure 2 displays the evolution of the ridge for  $n = 3$ . It can be observed that  $h$  has an inflexion point. It is located near  $x = 0$  at the beginning, and migrates towards large  $x$  as  $t$  increases, tending to reach the leading part of the ridge, where  $h$  approaches 1. It can be also noticed that the aspect ratio (height/width) of the ridge decreases with time. Qualitatively similar results are found for other values of  $n$ . In figure 3 we compare the profiles for  $n = 1, 3$  and  $10$  and for  $t = 0.3$  and  $t = 8$ . It can be observed that the larger is  $n$ , the narrower and higher is the ridge.

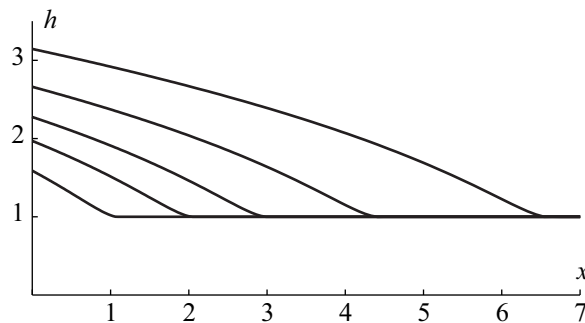


**Figure 2.** Numerical profiles for  $n = 3$  and  $t = 0.3, 1, 2, 4$  y  $8$ .

### 4. Self-similar behavior for $t \ll 1$

For small  $t$ , when  $h \approx 1$ , equation (2) can be linearized. To this end we seek a solution of the form

$$h(x, t) = 1 + t^{1/2} f(\psi), \quad \psi = \frac{x}{2\sqrt{t}}, \quad (6)$$

in which the elevation difference  $t^{1/2} f(\psi) \ll 1$ . Here the exponents of  $t$  in front of  $f$  and in the definition of  $\psi$  are both equal to  $1/2$ . This choice ensures that the linearized boundary condition at  $x = 0$  and the mass conservation do not depend on  $t$ , and implies that in this regime the height and the width of the ridge increase as  $t^{1/2}$  regardless of  $n$ . Notice however that  $n$  appears in the equation for  $f$ :

$$0 = f - \psi f' - 2^{-n} n (-f')^{n-1} f'', \quad (7)$$

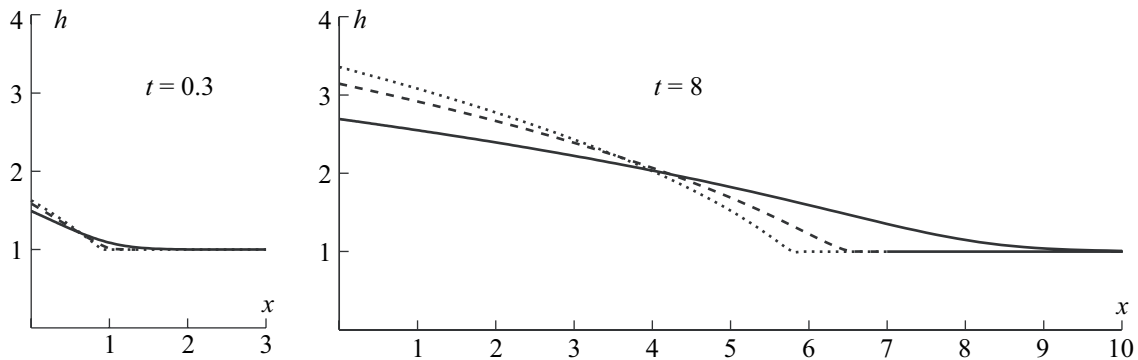


**Figure 3.** Numerical profiles at  $t = 0.3$  (left) and  $t = 8$  (right) for  $n = 1$  (full line), 3 (dashes) and 10 (points).

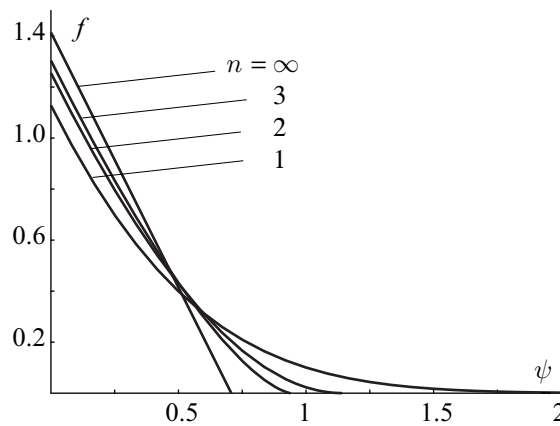


**Figure 4.** Profiles of  $f$  for  $t \ll 1$  with  $n = 1, 2, 3,$  and  $\infty$ .

so that the shape of the ridge depends on  $n$ .

The boundary conditions are  $f'(0) = -2$  and  $f(\infty) = 0$ . From the second of these conditions we obtain

$$f(0) = \frac{\sqrt{2}n}{n-1 + \sqrt{\frac{\pi}{2}}}.$$

In the limit  $n \rightarrow \infty$  the solution of (7) is  $f_\infty = \sqrt{2} - 2\psi$ . The solution for  $n = 1$  was obtained in [6] and is

$$f_1 = \frac{2e^{-\psi^2}}{\sqrt{\pi}} - 2\psi \operatorname{erfc}(\psi),$$

where  $\operatorname{erfc}(\psi) = 1 - \operatorname{erf}(\psi)$  is the complementary error function. For other values of  $n$  the function  $f$  is obtained by numerical integration. In figure 4 we show  $f(\psi)$  for different values of the rheological index. The maximum height of the ridge in the linear regime is given by

$$h_w = 1 + \frac{\sqrt{2}n}{n-1 + \sqrt{\frac{\pi}{2}}} t^{1/2}. \quad (8)$$

In figure 5 we show the evolution of the maximum elevation difference  $h_w - 1$ . It can be seen that for small  $t$  it tends to the self-similar behavior given by equation (8).

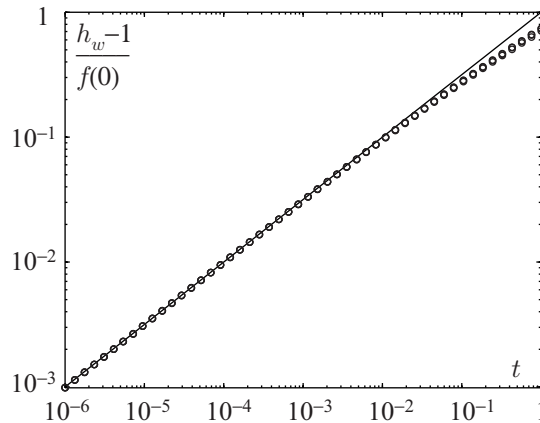


**Figure 5.** Evolution of the maximum height of the ridge. The full line corresponds to the scaling law  $t^{1/2}$  and the circles to the numerical solutions with  $n=1, 2$  and  $3$ .

Summarizing, in this regime the height and the width increase as  $t^{1/2}$  regardless of  $n$ , but  $h_w$  and the shape of the ridge depend on  $n$ .

### 5. Self-similar behavior for $t \gg 1$

For very large time the solution tends to another self-similar regime. To obtain it we seek a solution of the form  $h = t^\alpha F(\xi)$ , with  $\xi = x/t^\beta$ . Imposing the boundary condition at  $x = 0$  and assuming mass conservation, we find that  $\alpha = n/n_3$  and  $\beta = n_2/n_3$ , where  $n_2 = 1 + 2n$  and  $n_3 = 1 + 3n$ . Replacing in the differential equation for  $h$  and integrating once, we find the following differential equation for  $F$ :

$$F - F^{n_2} (-F')^n = A, \quad A = \text{const.} \quad (9)$$

By comparing this with the boundary condition at  $\xi = 0$  we find that  $A = 0$ . Then the solution of (9) is

$$F = \left( B - \frac{n_2}{n} \xi \right)^{n/n_2}, \quad \xi = \frac{x}{t^{n_2/n_3}}.$$

In consequence

$$h = t^{n/n_3} \left( B - \frac{n_2}{n} \frac{x}{t^{n_2/n_3}} \right)^{n/n_2}.$$

To find  $B$  we define  $x_f$  as the place where  $h = 0$ , and we obtain  $x_f = (nB/n_2)t^{n_2/n_3}$ . Since  $h \gg 1$  in the present regime,  $x_f$  can be called the “front” of the current. Next we impose  $\int_0^{x_f} h_t dx = 1$ , and we find  $B = (n_3/n)^{n_2/n_3}$ , so finally we obtain

$$h = h_w \left( 1 - \frac{x}{x_f} \right)^{n/n_2}, \quad (10)$$

with

$$h_w \equiv h(0) = \left( \frac{n_3}{n} t \right)^{n/n_3}, \quad x_f = \frac{n}{n_2} h_w^{n_2/n}. \quad (11)$$

In figure 6 we show this solution for different values of  $n$  at a given time.

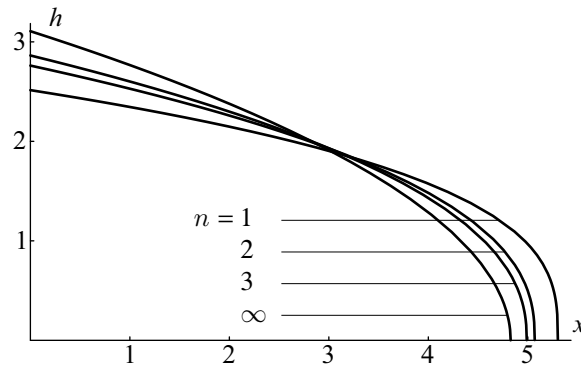


**Figure 6.** Self-similar solution (10–11) for  $t = 10$  with  $n = 1, 2$  y  $3$ , and in red for  $n \rightarrow \infty$ .

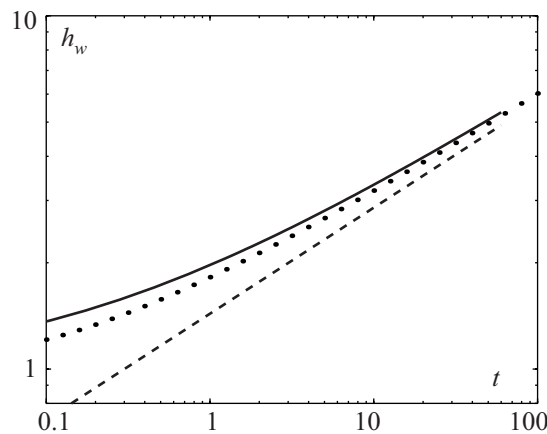


**Figure 7.** Evolution of maximum height of the ridge for  $n = 3$  and large  $t$ . The full line corresponds to the numerical solutions, the dashed line corresponds to equation (11) and the dotted line correspond to the quasi-self-similar solution.

A better approximation can be achieved by means of the quasi-self-similar approach [9; 10]. For this purpose we define the position of the front as the place where  $h = 1$ , we proceed as before, and  $B$  is obtained as the solution of the following equation:

$$B = \left( \frac{B}{t^{n/n_3}} + \frac{n_3}{n} \right)^{n_2/n_3}.$$

From this equation we find the following equations for  $h_w$  and  $x_f$  in place of (11):

$$h_w^{n_3/n} = h_w^{n_2/n} + \frac{n_3}{n} t, \quad x_f = \frac{n}{n_2} \left( h_w^{n_2/n} - 1 \right). \quad (12)$$

From these results one sees that for very large times the quasi-self-similar solution tends to agree with the self-similar one. Closed form expressions of  $h_w$  and  $x_f$  can only be obtained for  $n = 1$  and  $\infty$ , but they are very cumbersome and we shall not reproduce them here. In figure 7 we compare the values of  $h_w$  for  $n = 3$  from the numerical solution with those given by the self-similar and the quasi-self-similar solutions.

We can improve the description far from the crest if we follow an approach similar to that described in [6]. To this end, we look for a solution that satisfies  $F(\infty) = t^{-n/n_3}$  (to ensure that

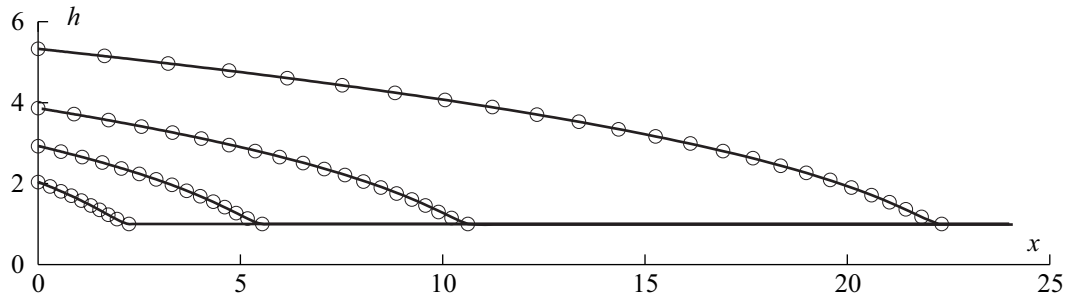


**Figure 8.** Comparison of the numerical profiles (lines) at  $t = 1.2, 6, 18$  and  $60$  with the profiles of the rescaled solution (circles) from (15) in which  $h_w$  is given by the numerical solutions and  $n = 3$ .

$h(\infty) = 1$ ), sacrificing the condition at  $\xi = 0$ . Next we set  $\alpha = n/n_3$ ,  $\beta = n_2/n_3$  and integrate the leading term of the differential equation for  $f$ . The resulting equation is again (9), but now  $A \neq 0$ , and the solution is given in implicit form by

$$\xi = \frac{n}{2(1+n)} \left( -\frac{F^{1+n_2}}{A} \right)^{1/n} {}_2F_1 \left[ \frac{1+n_2}{n}, \frac{1}{n}; \frac{1+n_3}{n}; \frac{F}{A} \right] + c. \quad (13)$$

Here  $c = \text{const.}$  and  ${}_2F_1[a, b; c; w]$  is the hypergeometric function. Now we allow the integration constants  $A$  and  $c$  to depend weakly on  $t$ . To satisfy the condition at infinity we set  $A = t^{-n/n_3}$ , and to find  $c$  we require that  $h = h_w$  when  $x = 0$ . The solution is then

$$x = \int_h^{h_w} \left( \frac{s^{2+n}}{s-1} \right)^{1/n} ds. \quad (14)$$

Notice that this integral can be expressed in terms of the incomplete Beta function, although there is no advantage in doing that. Of course the solution (14) does not satisfy the boundary condition at  $x = 0$  given in (5). However it is possible to modify (14) in order to fulfill this condition by rescaling  $x$ . This rescaling is needed to ensure that  $h'(0)$  has the appropriate value, and can be achieved multiplying the r.h.s. of (14) by the factor  $[(h_w - 1)/h_w]^{1/n}$ . We then find

$$x = \left( \frac{h_w - 1}{h_w} \right)^{1/n} \int_h^{h_w} \left( \frac{s^{2+n}}{s-1} \right)^{1/n} ds. \quad (15)$$

So far we have not yet specified  $h_w$ . If we employ the value of  $h_w$  obtained from the numerical solutions the agreement is excellent, even for  $t \approx 1$ , as can be appreciated in figure 8. For  $t$  not very large the  $h_w$  from (12) corresponding to the quasi-self-similar solution differs only by a few percent (the difference tends to increase with  $n$ ) from the exact value (see figure 7). Then if high precision is not needed, one can use the rescaled solution (15) with the value of  $h_w$  given by (12).

## 6. Conclusions

As in the Newtonian case the evolution of the ridge takes place in two stages. In the beginning the profile  $h(x, t)$  looks like the self-similar solution (6–7). Later on  $h(x, t)$  tends to the solution (10–11). The transition between these stages occurs around  $t \approx 1$ , and corresponds to the migration of the inflexion point of  $h(x, t)$ , that initially is close to  $x = 0$ , and approaches  $x_f$



as  $t \rightarrow \infty$ . During the first stage the width and the relief increase as  $t^{1/2}$ . But as the height becomes large, the mass that is added mostly goes to increase the width of the ridge, which then grows faster than the height.

Summarizing, in the formation of a ridge there are two self-similar regimes. In the linear regime, when  $t \lesssim 0.1$ , the profile is given by (6–7) and the horizontal and vertical scales increase as  $t^{1/2}$ . As  $n$  varies the shape of the ridge varies between  $f_1$  for  $n = 1$  and a triangle for  $n \rightarrow \infty$ . In the large time regime (when  $t \gtrsim 10$ ) the profile is given by (10–11) and the height scales as  $t^{n/(1+3n)}$ , while the width increases as  $t^{(1+2n)/(1+3n)}$ . These scaling laws coincide with those previously derived in [1] by means of dimensional analysis. For fixed  $t$ , as  $n$  increases, the peak of the ridge becomes more pronounced and its average slope becomes larger.

The analogy between the present results and those derived for a Newtonian liquid [6] can be traced to the fact that the constitutive relation (1) introduces a single-dimensional parameter ( $A$ ) into the problem, as in the case of a Newtonian liquid (the viscosity coefficient). In both instances this dimensional parameter can be scaled out by an appropriate definition of the dependent variable, and thus does not appear in the final governing equations. For this reason one finds similarity solutions whenever the analogous Newtonian problem is self-similar. The dimensionality of  $A$  depends on the rheological index  $n$  and, as a consequence, the large time scaling laws have rheology-dependent exponents. It is interesting to observe that these dependences are weak. However, the differences between Newtonian and non-Newtonian flows are quantitatively significant.

### Acknowledgments

We acknowledge grants PIP 5377 from CONICET, X031 from Universidad de Buenos Aires and PICTR 2002-00094 and PICTO 21360 from ANPCYT.

### References

- [1] Gratton J 1989 *J. Geophys. Res.* **94** 15627–15634
- [2] England P and McKenzie D 1982 *Geophysical Journal International* **70** 295–321
- [3] England P and McKenzie D 1983 *Geophysical Journal International* **73** 523–532
- [4] Medvedev S E and Podladchikov Y Y 1999 *Geophysical Journal International* **136** 567–585
- [5] Medvedev S E and Podladchikov Y Y 1999 *Geophysical Journal International* **136** 586–608
- [6] Perazzo C A and Gratton J 2008 *Physics of Fluids* **20** 043103
- [7] Ranalli G and Murphy D 1987 *Tectonophysics* **132** 281–295
- [8] Gratton J, Minotti F and Mahajan S M 1999 *Phys. Rev. E* **60** 6960–6967
- [9] Diez J A, Gratton R, Thomas L P and Marino B 1994 *J. Colloid Interface Sci.* **168** 15–20
- [10] Gratton R, Diez J A, Thomas L P, Marino B and Betelú S 1996 *Phys. Rev. E* **53** 3563–3572